ELSEVIER

Journal of Power Sources 112 (2002) 428–434

JOURNAL OF POWER SOURCES

www.elsevier.com/locate/jpowsour

Structural characteristics of nickel hydroxide synthesized by a chemical precipitation route under different pH values

Quansheng Song[a,b,*], Zhiyuan Tang[a], Hetong Guo[a], S.L.I. Chan[b]

[a]*Department of Applied Chemistry, College of Chemical Engineering, Tianjin University, Tianjin 300072, PR China*
[b]*Department of Materials Science and Engineering, National Taiwan University, Taipei 106, Taiwan*

Received 18 March 2002; received in revised form 4 July 2002; accepted 25 July 2002

Abstract

The effects of precipitation pH values on the microstructural characteristics of nickel hydroxide materials synthesized by a chemical precipitation method have been studied. The relationship between structural characteristics and electrochemical activity of nickel hydroxide was also examined. The structural characteristics of the synthesized β-$Ni(OH)_2$, such as degree of crystallinity, crystalline lattice disorders, crystallite size and crystal growth orientation were strongly related to the pH values of the chemical precipitation reaction. The amounts of SO_4^{2-}, CO_3^{2-} and H_2O adsorbed in crystals, and the thermal stability of the β-$Ni(OH)_2$ also depended on the pH. Under relatively high pH values, the synthesized nickel hydroxide materials possessed a reduced crystallite size and lower thermal stability, more crystalline defects and a higher Ni composition. All these characteristics were likely to improve the electrochemical activity of nickel hydroxide.

Keywords: Nickel hydroxide; Alkaline storage batteries; Structural characteristics; Chemical precipitation reaction

1. Introduction

Nickel hydroxide is the positive electrode active material in rechargeable alkaline batteries (e.g. Ni/Fe, Ni/Zn, Ni/Cd, Ni/H_2 and Ni/MH). The alkaline nickel batteries are usually positive limited, meaning that the material utilization of nickel hydroxide dictates the amount of capacity that can be stored on charging and the amount of capacity that can be recovered during discharging. With the rapid progress of research and development of hydrogen storage alloy materials and nickel/metal hydride batteries (Ni/MH) in recent years, the preparation of high-performance nickel hydroxide electrode materials becomes a critical issue. The practical importance of nickel hydroxide structure and its electrochemical properties is not only limited to battery application, since nickel hydroxide or nickel oxide electrodes also find applications in fuel cells, electrochemical capacitors, electrolyzers, electrosynthetic cells and electrochromic devices.

It is well established that nickel hydroxide exists in two polymorphic forms, α- and β-$Ni(OH)_2$, which on charging (oxidation) transform to γ- and β-NiOOH, respectively [1,2]. These structures and their modifications are probably hydrated to some extent. Among the different polymorphic modifications of nickel hydroxide, the β-form is widely used as the positive electrode precursor materials in all nickel based secondary cells [3]. β-$Ni(OH)_2$ crystallizes with a hexagonal brucite structure, with an inter-sheet distance of $c_0 = 4.60$ Å and a Ni–Ni atom distance of $\alpha_0 = 3.12$ Å. With its high stability in strong alkaline electrolyte, β-$Ni(OH)_2$ is often selected as a discharged-state active material in the fabrication of nickel electrode. β-$Ni(OH)_2$ has a good reversibility when charged to β-NiOOH, which has a similar layered structure with lattice parameters $c_0 = 4.85$ Å and $\alpha_0 = 2.82$ Å. On prolonged charging, however, β-NiOOH is converted to γ-NiOOH, which has an expanded c_0 parameter of 7 Å. γ-NiOOH can also be formed under conditions of overcharging, high rate charging, or high electrolyte concentrations [4]. The conversion of β-NiOOH to γ-NiOOH is accompanied by a large volumetric change and this may result in the swelling of the nickel electrode and the drying of electrolyte in the separator. Consequently, the formation of γ-NiOOH considerably damages the nickel electrode and induces immature cell failure. In addition, it has been reported recently that the cause of the memory effect in alkaline secondary batteries is also related to the formation of γ-NiOOH [5]. In order to inhibit the formation of γ-NiOOH, some additives, such as Co, Cd and Zn have been used in the fabrication of nickel electrode [6].

* Corresponding author. Tel.: +886-2-23631531; fax: +886-2-23634562.
E-mail address: qshsong@ccms.ntu.edu.tw (Q. Song).

0378-7753/02/$ – see front matter
PII: S0378-7753(02)00396-8

Another polymorphic form of nickel hydroxide, α-$Ni(OH)_2$, with a nearly identical c_0 parameter (7.6 Å) to that of γ-NiOOH, can be transformed to γ-NiOOH phase reversibly without mechanical deformation or constraints. The α/γ couple is also expected to exhibit a higher theoretical capacity relative to that of the β(II)/β(III) couple. This can be attributed to the fact that more than one electron may be exchanged per nickel atom during the α–γ phase transformation, owing to a higher oxidation state (3.5 or higher) of nickel in γ-NiOOH [7,8]. Thus the α/γ couple is theoretically envisaged to have a superior electrochemical performance as compared to the β(II)/β(III) couple. However, α-$Ni(OH)_2$ is thermodynamically unstable in strong alkaline medium and rapidly transforms to β-$Ni(OH)_2$. In order to stabilize the structure of α-$Ni(OH)_2$, partial substitutions of over 20% of Co, Fe, Al, Zn and Mn for Ni in nickel hydroxide have been studied [9–13]. The development of reliable routes to the synthesis and stabilization of α-$Ni(OH)_2$ is a major scientific challenge for realizing the advantages of the α/γ couple in the operational conditions of an alkaline secondary battery.

It is widely accepted that the nickel electrode works as an insertion electrode for protons, the redox reaction of Ni(II)/Ni(III) in alkaline media can be expressed as:

$$NiOOH + H_2O + e^- \rightleftarrows Ni(OH)_2 + OH^- \quad (1)$$

which is believed to be a solid-state proton intercalation and de-intercalation reaction [14]. In the charge/discharge process, the proton insertion into and desertion from the hexagonal structure of nickel hydroxide occur reversibly, and the crystal structure of nickel hydroxide is maintained. The electrochemical activity of nickel hydroxide materials can be improved by increasing the proton diffusion coefficient in nickel hydroxide, which is closely related to its microstructure. Studies [3,15] have shown that for nickel hydroxide with a smaller crystallite size and more crystalline defects, it possesses a higher chemical proton diffusion coefficient, and this will diminish the concentration polarization of protons during charge/discharge, leading to a better charge/discharge cycling behavior. The microstructure of nickel hydroxide is determined by both composition (e.g. doping elements in nickel hydroxide) and processing. Microstructure control by changing the preparation techniques and synthesis parameters has received particular attention for being effective on the improvement of the electrochemical properties of nickel hydroxide materials. Several synthesis methods of nickel hydroxide have been developed, such as chemical precipitation [16], electrochemical deposition or electrosynthesis [17], and chimie douce technique [18]. Among these synthesis routes, the wet chemical precipitation method is widely used to produce spherical nickel hydroxide powder. This powder can be used to fabricate Ni-foam pasted-type nickel electrodes, which are now commercially available for Ni/MH batteries [19].

The microstructural characteristics of nickel hydroxide materials synthesized by the chemical precipitation method are closely related to the synthesis process parameters, such as concentration of reagent solutions, reaction temperature, pH value, addition amount of complexing agent, doping elements, etc. [20]. Among these synthesis parameters, the precipitation pH value is a key factor that affects the crystal and chemical structure characteristics of nickel hydroxide. This paper reports our study on the influence of chemical precipitation reaction pH values on the structure of nickel hydroxide materials. Powder X-ray diffraction (XRD), infrared (IR) spectroscopy, thermogravimetric (TG) and differential thermogravimetric (DTG) analyses have been employed to characterize the structure and amounts of SO_4^{2-}, CO_3^{2-} and H_2O adsorbed in the materials. The relationship between structural characteristics and electrochemical activity of nickel hydroxide has also been investigated.

2. Experimental

2.1. Preparation of nickel hydroxide materials

$Ni(OH)_2$ was synthesized via an aqueous solution complexation–precipitation route. In the synthesis, $NiSO_4$ and NaOH were used as reagents, with NH_4OH as a complexing agent. Pre-determined amounts of $NiSO_4$, NaOH and aqueous ammonia were fed by dripping into a reactor with vigorous stirring. During the precipitation process, the temperature of the reactor was controlled at $60 \pm 1\ ^\circ C$. The pH of the suspension in the reactor was maintained by adjusting the feed rates of the reagent solutions, and the pH value was closely monitored by a digital precise pH-meter. In order to remove the excess of SO_4^{2-}, OH^- and NH_4^+ ions in the product, the blue–green precipitate was repeatedly washed and filtered to neutral pH with distilled water. The precipitate was then dried to constant weight under vacuum. Finally the dried precipitate was pulverized to obtain the $Ni(OH)_2$ samples and stored for structural analysis. To study the effect of precipitation pH values on the structure of nickel hydroxide, the $Ni(OH)_2$ samples were prepared using three different pH values (sample A: pH = 7.25; sample B: pH = 10.50; sample C: pH = 11.50). All other precipitation parameters were kept unchanged.

2.2. Structure characterization of nickel hydroxide materials

XRD patterns of the $Ni(OH)_2$ samples were recorded on a RIGAKU X-ray diffractometer using Cu Kα radiation ($\lambda = 1.542$ Å), with a scanning rate of 4° (2 θ) per minute and a scanning range of 14–80° (2 θ). IR spectra were obtained using a Bio-RAD FTS-3000 infrared spectrometer in KBr pellets. TG and DTG analyses were carried out with a SHIMADZU TGA-50 thermal analyzer, with a heating rate of 10 °C/min in N_2.

3. Results and discussion

3.1. Discharge capacities of the $Ni(OH)_2$ samples

The three nickel hydroxide samples have been used as the active material for pasted foam-nickel electrodes with cobalt powder as a conductive additive [20]. Charge/discharge cycling tests of the nickel electrodes showed that the specific discharge capacities were 180, 217 and 245 mAh/g-$Ni(OH)_2$ for samples A, B and C respectively. Thus the nickel hydroxide samples synthesized at relatively high pH values are expected to have a better electrochemical activity.

3.2. XRD patterns

XRD patterns of $Ni(OH)_2$ samples A–C are presented in Fig. 1. The characteristic diffraction peaks at (0 0 1)($d_{4.60}$), (1 0 0)($d_{2.70}$), (1 0 1)($d_{2.34}$), (1 0 2)($d_{1.76}$), (1 1 0)($d_{1.56}$) and (1 1 1)($d_{1.48}$) show that all these samples have a crystal structure of β-type $Ni(OH)_2$. Some disorders in the crystal lattice, which are characterized by the full-width of half-maximum intensity (FWHM) of the (0 0 1), (1 0 1) and (1 0 2) reflection lines [8,10], can also be found. The interlayer distance c_0 of a brucite-type structure of nickel hydroxide is represented by the $d_{0\,0\,1}$ value. The $d_{1\,0\,0}$ or $d_{1\,1\,0}$ value corresponds to the Ni–Ni distance α in the layers of nickel hydroxide, where $\alpha = [2/\sqrt{3}]d_{1\,0\,0}$ or $2d_{1\,1\,0}$ [14,23]. Though the samples A–C have the same β-$Ni(OH)_2$ basic structure, their detailed microstructural characteristics are considerably different as revealed in the XRD patterns Fig. 1:

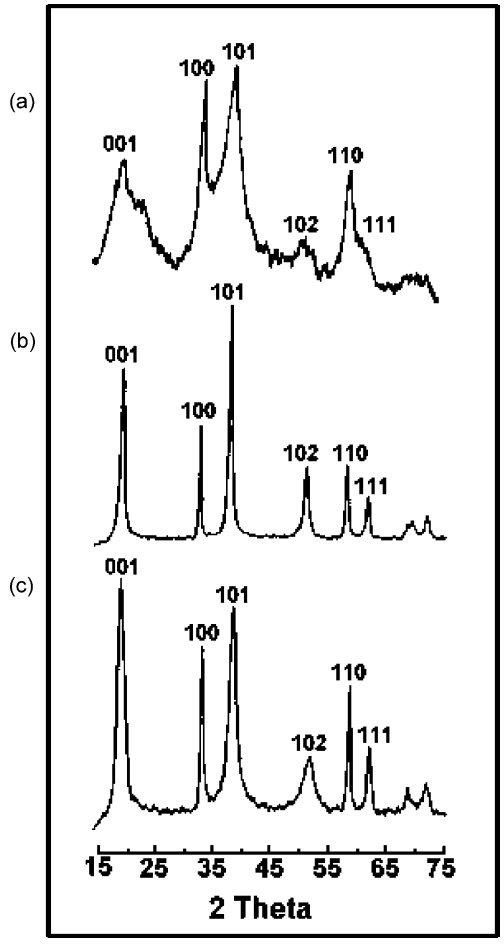

Fig. 1. XRD patterns of $Ni(OH)_2$ samples synthesized at different pH values: (a) sample A, pH = 7.25; (b) sample B, pH = 10.50; (c) sample C, pH = 11.50.

1. The peaks corresponding to all the reflections in the XRD pattern of sample A are noticeably broadened and/or split as compared to those in the patterns of samples B and C. This indicates that the as-prepared sample A is very poorly crystallized. For the samples B and C, which are synthesized with higher precipitation pH values, the XRD patterns show sharper reflection peaks, indicative of an increased degree of ordering and crystallinity for these samples.
2. For the well-crystallized samples B and C, the peaks in the XRD patterns are not uniformly broadened. A larger degree of broadening (FWHM) of the peaks corresponding to the (0 0 1), (1 0 1) and (1 0 2) reflections is obtained, while the broadening for the peaks corresponding to the (1 0 0) and (1 1 0) is smaller. The exceptional broadening of the (0 0 1), (1 0 1) and (1 0 2) reflection lines in the XRD patterns of nickel hydroxide materials may be attributed to [21,22]: (i) crystallite size effects; (ii) increased degree of disordering on account of the existence of crystalline defects, such as stacking faults/growth faults and proton vacancies, or the adsorption of inorganic species (water and anions); and (iii) the presence of other polymorphic modifications as interstratified phases. It can also be found that the FWHMs of the (0 0 1), (1 0 1) and (1 0 2) reflections in the XRD pattern of sample C are larger than those for sample B. This suggests that the crystallite size of $Ni(OH)_2$ powder sample C synthesized at a relatively higher pH value tends to decrease and the amount of crystalline defects tends to increase, thus resulting in a larger FWHMs for sample C. As described in the introduction, nickel hydroxide with a smaller crystallite size and more structural defects shows a higher chemical proton diffusion coefficient, giving an excellent charge/discharge cycling behavior.
3. The crystal growth orientation of the chemically precipitated nickel hydroxide materials also depends on pH values. The (1 0 1) reflection is the most intensive in the XRD patterns of samples A and B, while the (0 0 1) reflection is the most intensive in that of sample C. This indicates that the crystal growth/stacking speed of nickel hydroxide in the direction of "*c*-axis" of layered structure increases with pH values.

3.3. IR spectra

To further support the XRD study, Fig. 2 gives the infrared spectra of the as-prepared samples A–C. The infrared

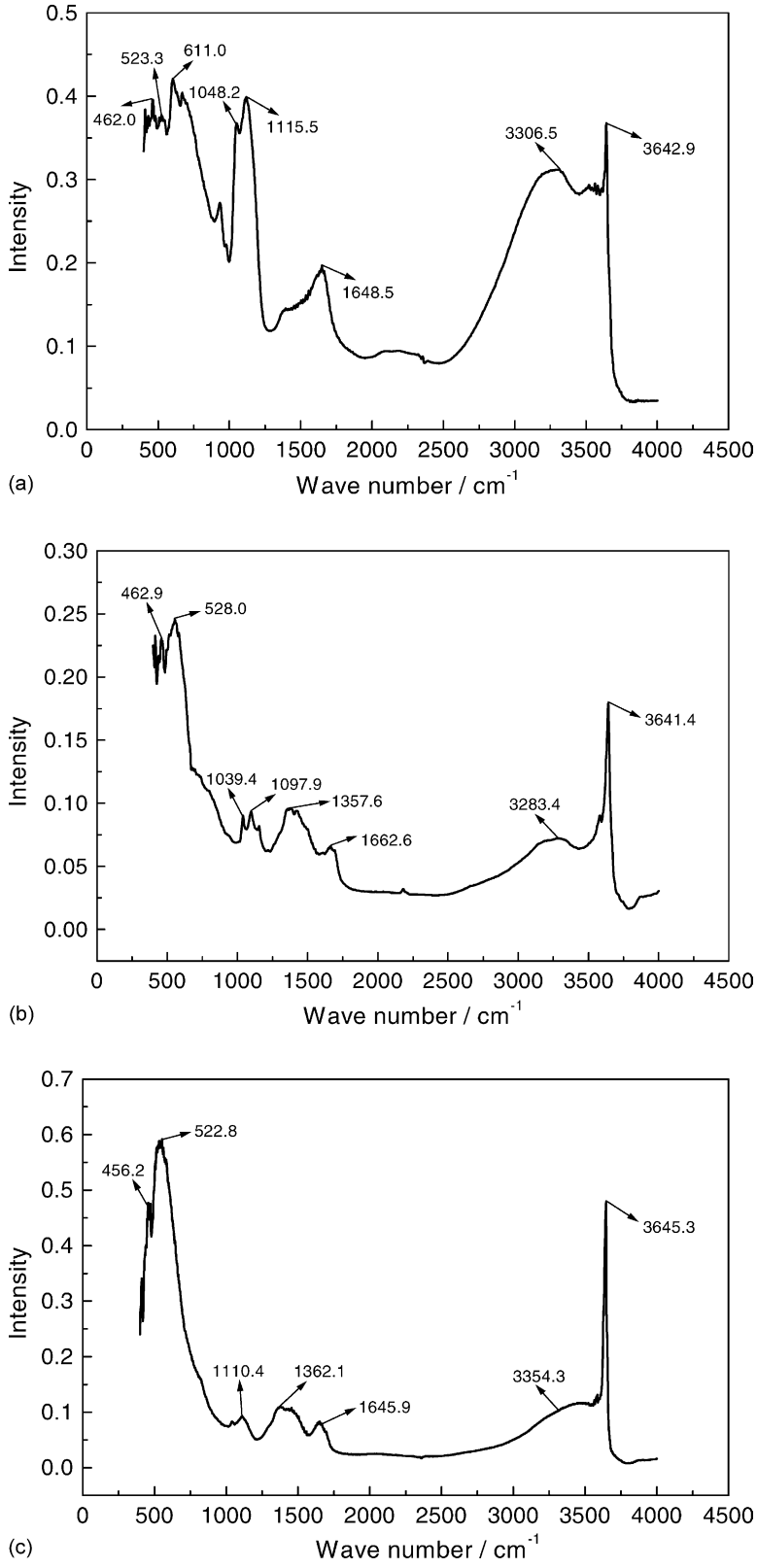

Fig. 2. IR spectra of $Ni(OH)_2$ samples synthesized at different pH values: (a) sample A, pH = 7.25; (b) sample B, pH = 10.50; (c) sample C, pH = 11.50.

spectra are useful to probe the short-range structure of $Ni(OH)_2$, as contrast to the X-ray diffraction patterns which result from long-range phenomena. The IR spectra in Fig. 2 also verify that the samples A–C can be characterized as β-type $Ni(OH)_2$, on the ground that: (i) a narrow and strong band at 3642 cm^{-1} owing to the ν(OH) stretching vibration, which indicates OH groups in a free configuration; (ii) a strong band at 520 cm^{-1} corresponding to the hydroxyl groups' lattice vibration δ(OH); and (iii) a band with weak intensity around 460 cm^{-1} resulting from the Ni–O lattice vibration ν(Ni–O) [16,18].

A few distinguishing features of the IR spectra for these samples can also be revealed in Fig. 2:

1. For the samples A–C, the intensity of the band assigned to the ν(OH) stretching vibration in the IR spectra is noticeably increased with increasing pH values. That is, the degree of crystallinity of nickel hydroxide is improved with an increase of pH values. This result is in good agreement with that obtained by XRD.
2. The appearance of the large bands around 3300 and 1650 cm^{-1}, because of the $\nu(H_2O)$ stretching vibration and the $\delta(H_2O)$ bending vibration of water molecules, indicates the presence of a certain amount of water molecules adsorbed on the nickel hydroxide materials. The intensity of these two bands resulting from water molecules decreases with increasing pH values, suggesting that the content of the adsorbed water in $Ni(OH)_2$ samples decreases with an increase in pH values. This result is further corroborated by TG and DTG studies.
3. The different bands observed in the range of 1500–800 cm^{-1} can be attributed to the presence of several ions, such as carbonate and/or sulphate. The bands around 1100, 1040 and 610 cm^{-1} in the IR spectra are characteristics of SO_4^{2-} anions; and the band at 1360 cm^{-1} corresponds to the presence of CO_3^{2-} anions. The SO_4^{2-} anions originate from the metal salt solution ($NiSO_4$) used for the precipitation, and the CO_3^{2-} anions are believed to come from the dissolution of CO_2 in the air during the synthesis. These anions are mainly adsorbed on the nickel hydroxide grain surface because the value of c_0 parameter (4.6 Å) of β-$Ni(OH)_2$ does not allow the presence of the anions intercalated between the slabs of $Ni(OH)_2$. Especially for the intercalation of SO_4^{2-}, an interslab distance close to 9 Å will be required [11,23]. In comparison with that of the IR spectra for samples B and C, the intensity of the SO_4^{2-} bands in the IR spectra of sample A is the largest, and the CO_3^{2-} bands are almost absent. With an increase in pH values, the intensity of the SO_4^{2-} bands in the IR spectra of samples B and C decreases, but the CO_3^{2-} bands become readily apparent. The intensity of the CO_3^{2-} bands also increases with increasing pH values. With an increase in pH values, the spontaneous exchange of SO_4^{2-} for CO_3^{2-} ions can occur in agreement with the adsorption selectivity of the anions, as the preference order of the anions adsorption in $Ni(OH)_2$ is: $CO_3^{2-} \gg SO_4^{2-} > Cl^- > NO_3^-$ [18]. This suggests that the content of SO_4^{2-} in the $Ni(OH)_2$ sample synthesized at a low pH value is relatively high, while the amount of CO_3^{2-} in the $Ni(OH)_2$ sample synthesized at a high pH value is relatively large.
4. The intensity of the band assigned to the δ(OH) lattice vibration noticeably increases with increasing pH values. This means that the $Ni(OH)_2$ concentration (i.e. Ni composition) in the synthesized materials is increased at high pH values. This result is also confirmed by TG studies.

3.4. TG and DTG analyses

The amount of water in the nickel hydroxide materials plays an important role in the crystal structure and the electrochemical properties of $Ni(OH)_2$. For example, it was reported that the water content for β-$Ni(OH)_2$ varied from 0 to 0.3 molar fraction (moles of H_2O per mole of $Ni(OH)_2$), and for α-$Ni(OH)_2$ the water content varied from 0.3 to 0.7 molar fraction, depending upon the preparative experimental conditions [24]. In this work, TG and DTG analyses have been used to investigate the water content and the dehydration reactions of nickel hydroxide. TG and DTG curves for $Ni(OH)_2$ samples A–C are shown in Fig. 3.

For sample A synthesized at pH = 7.25, the TG and DTG curves reveal two obvious weight loss regions: a first region below 250 °C (between room temperature and 250 °C); and a second region between 250 and 450 °C. These two regions are distinctly exhibited in DTG curve as two peaks: one broad peak corresponding to the first region; and the other, a sharp, intense peak corresponding to the second region. The second peak in DTG curve is somewhat split, this may be attributed to the relatively large SO_4^{2-} content in $Ni(OH)_2$ crystals synthesized at a low pH. Above 450 °C, no appreciable weight change is observed in TG and DTG curves. Two categories of chemical reactions are postulated which correspond to the observed steps of weight loss in the experiments. One process is the dehydration (Eq. (2)) which corresponds to the first weight loss below 250 °C; and the other is the decomposition of nickel hydroxide to nickel oxide (Eq. (3)), which corresponds to the second weight loss above 250 °C.

Dehydration reaction:

$$Ni(OH)_2 \cdot X_{ads}H_2O \rightarrow Ni(OH)_2 + XH_2O \quad (2)$$

Decomposition reaction:

$$Ni(OH)_2 \rightarrow NiO + H_2O \quad (3)$$

Several investigators have noted that the water in nickel hydroxide can either be adsorbed or structurally bonded in between the $Ni(OH)_2$ lattices [23,24]. Structurally bonded water (i.e. intercalated water) thereby alters the interplanar distances in the crystal structure, resulting in an expansion of

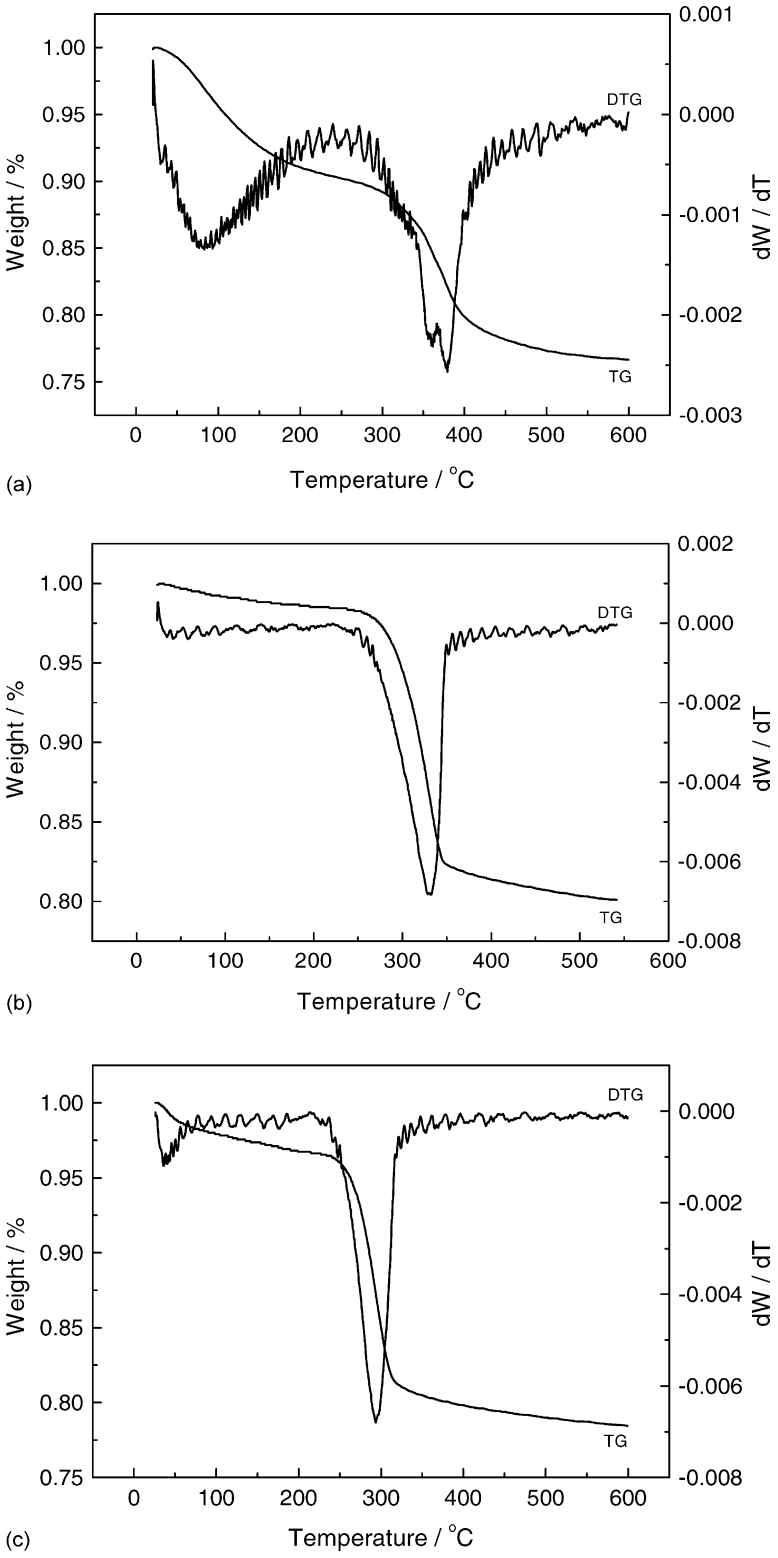

Fig. 3. TG and DTG plots for $Ni(OH)_2$ samples synthesized at different pH values: (a) sample A, pH = 7.25; (b) sample B, pH = 10.50; (c) sample C, pH = 11.50.

"*c*-axis" from 4.6 Å for β-$Ni(OH)_2$ to approximately 8 Å for fully hydrated α-$Ni(OH)_2$. In the present study, there is no expansion of the "*c*-axis" in the hydrated β-phase, thus indicating the presence of adsorbed water only, without any structurally bonded water in β-$Ni(OH)_2$. As shown by XRD and IR studies, all the batches of nickel hydroxide synthesized in this study have a β-phase structure. Water molecules can only be adsorbed in these materials, as the small

interslab distance ($c_0 = 4.6$ Å) of β-$Ni(OH)_2$ excludes the intercalation of such water molecules.

In Eq. (2), the $H_2O/Ni(OH)_2$ molar ratio X_{ads} can be estimated from the weight loss corresponding to the dehydration reaction, and the nominal stoichiometric compositions of the nickel hydroxide samples are obtained. The theoretical weight loss corresponding to the decomposition reaction (Eq. (3)) is 19.49%, and the practical weight loss corresponding to this reaction, which can be estimated from the second weight loss steps of TG curves, are 12.09, 17.65 and 17.42% for $Ni(OH)_2$ samples A, B and C, respectively. This indicates that the $Ni(OH)_2$ concentration (i.e. Ni composition) is higher in samples B and C than in sample A. The deviations between the practical and theoretical weight loss may be attributed to the SO_4^{2-} and CO_3^{2-} adsorbed in these materials, as revealed by the IR study.

Compared with the TG and DTG results of sample A, the experimental results for samples B and C show some distinguishing features:

1. With an increase in pH values, the height of the first weight loss steps in TG curves of samples B and C is reduced. Correspondingly the first peaks in DTG curves for these samples almost disappear. Meanwhile, the height of the second weight loss steps in TG curves increases with increasing pH values. Thus, the second peaks in DTG curves for samples B and C become more significant and sharper. The increase in the height of the weight loss steps means that the weight loss is increasing. This result shows that the water content in $Ni(OH)_2$ samples B and C is relatively lower as compared to that in sample A. The X_{ads} values for three $Ni(OH)_2$ samples A, B and C are found to be 0.56, 0.074 and 0.17, respectively.
2. With increasing pH values, the slopes of the second weight loss steps in TG curves increase. The temperatures corresponding to the decomposition reaction peaks in DTG curves also lower gradually, giving readings of 379, 330 and 294 °C, respectively, for samples A, B and C. The increase in the slopes of the weight loss steps means that the decomposition reaction of the $Ni(OH)_2$ samples speeds up. This indicates that with an increasing precipitation pH, the synthesized $Ni(OH)_2$ materials become less stable thermally, as reflected by a higher decomposition reaction rate and lower decomposition temperature. That is, the sample C synthesized at a high pH value has the lowest thermal stability as compared to that of samples A and B. The XRD measurement results also show that the crystallite size of samples C is smaller. Thus, it is found that $Ni(OH)_2$ materials with a smaller crystallite size possess a lower decomposition temperature and a higher decomposition rate. Such a relationship between the decomposition temperature and the crystallite size of nickel hydroxide materials has also been observed by Watanabe et al. [15]. So the lowering of the thermal stability is also likely to be beneficial to the electrochemical activity of nickel hydroxide.

4. Conclusions

It has been confirmed that the nickel hydroxide materials synthesized by a chemical precipitation method were crystalline β-$Ni(OH)_2$ with a brucite-type structure and a hexagonal unit cell. The precipitation pH value was found to be the key factor that affected the crystal and chemical structure characteristics of nickel hydroxide. It was shown that the structural characteristics of β-$Ni(OH)_2$, such as degree of crystallinity, crystalline lattice disorders, crystallite size and crystal growth orientation were strongly related to the pH values of the chemical precipitation reaction. The amounts of SO_4^{2-}, CO_3^{2-} and H_2O adsorbed in crystals, and the thermal stability of β-$Ni(OH)_2$ also depended on the pH. Under relatively high pH values, the synthesized nickel hydroxide materials possessed a reduced crystallite size and lower thermal stability, more crystalline defects and a higher Ni composition. All these characteristics were likely to be advantageous to the improvement of electrochemical activity of nickel hydroxide.

References

[1] P. Olive, J. Leonardi, J.F. Laurent, C. Delmas, J.J. Braconnier, M. Figlarz, F. Fievet, A. Guibert, J. Power Sources 8 (1982) 229.
[2] B.C. Cornilsen, X.Y. Shan, P.L. Loyselle, J. Power Sources 29 (1990) 453.
[3] R.S. Jayashree, P.V. Kamath, G.N. Subbanna, J. Electrochem. Soc. 147 (2000) 2029.
[4] D. Singh, J. Electrochem. Soc. 145 (1998) 116.
[5] Y. Sato, S. Takeuchi, K. Kobayakawa, J. Power Sources 93 (2001) 20.
[6] M. Oshitani, T. Takayama, K. Takashima, S. Tsuji, J. Appl. Electrochem. 16 (1986) 403.
[7] V.G. Kumar, N. Munichandraiah, P.V. Kamath, A.K. Shukla, J. Power Sources 56 (1995) 111.
[8] P.V. Kamath, M. Dixit, L. Indira, A.K. Shukla, V.G. Kumar, N. Munichandraiah, J. Electrochem. Soc. 141 (1994) 2956.
[9] C. Faure, C. Delmas, P. Willmann, J. Power Sources 36 (1991) 497.
[10] L. Indira, M. Dixit, P.V. Kamath, J. Power Sources 52 (1994) 93.
[11] L. Demourgues-Guerlou, C. Denage, C. Delmas, J. Power Sources 52 (1994) 269.
[12] L. Demourgues-Guerlou, C. Delmas, J. Power Sources 52 (1994) 275.
[13] M. Dixit, P.V. Kamath, J. Gopalakrishnan, J. Electrochem. Soc. 146 (1999) 79.
[14] K. Watanabe, N. Kumagai, J. Power Sources 76 (1998) 167.
[15] K. Watanabe, T. Kikuoka, N. Kumagai, J. Appl. Electrochem. 25 (1995) 219.
[16] P.V. Kamath, G.N. Subbanna, J. Appl. Electrochem. 22 (1992) 478.
[17] R.S. Jayashree, P.V. Kamath, J. Power Sources 93 (2001) 273.
[18] L. Demourgues-Guerlou, C. Delmas, J. Power Sources 45 (1993) 281.
[19] I. Munehisa, A. Norikatsu, Eur. Patent No. EP 0523284 (1993).
[20] Q.S. Song, Ph.D. Dissertation, Tianjin University, PR China, 2000.
[21] C. Tessier, P.H. Haumesser, P. Bernard, C. Delmas, J. Electrochem. Soc. 146 (1999) 2059.
[22] S. Deabate, F. Fourgeot, F. Henn, J. Power Sources 87 (2000) 125.
[23] C. Faure, C. Delmas, M. Fouassier, J. Power Sources 35 (1991) 279.
[24] B. Mani, J.P. Neufville, J. Electrochem. Soc. 135 (1988) 800.